

α decay of $^{180,181}\text{Pb}$

A. N. Andreyev,^{1,2} S. Antalic,³ D. Ackermann,⁴ T. E. Cocolios,¹ V. F. Comas,⁴ J. Elseviers,¹ S. Franchoo,⁵ S. Heinz,⁴ J. A. Heredia,⁴ F. P. Heßberger,⁴ S. Hofmann,^{4,6} M. Huyse,¹ J. Khuyagbaatar,⁴ I. Kojouharov,⁴ B. Kindler,⁴ B. Lommel,⁴ R. Mann,⁴ R. D. Page,⁷ S. Rinta-Antilla,⁷ P. J. Sapple,⁷ Š. Šáro,³ P. Van Duppen,¹ M. Venhart,¹ and H. V. Watkins⁷

¹*Instituut voor Kern- en Stralingsfysica, K. U. Leuven, University of Leuven, B-3001 Leuven, Belgium*

²*School of Engineering and Science, University of the West of Scotland, Paisley PA1 2BE, United Kingdom*

³*Department of Nuclear Physics and Biophysics, Comenius University, Bratislava SK-84248, Slovakia*

⁴*GSI Helmholtzzentrum für Schwerionenforschung GmbH, D-64291 Darmstadt, Germany*

⁵*IPN Orsay, F-91406 Orsay Cedex, France*

⁶*J. W. Goethe-Universität, D-60054 Frankfurt, Germany*

⁷*Department of Physics, Oliver Lodge Laboratory, University of Liverpool, Liverpool L69 7ZE, United Kingdom*

(Received 27 June 2009; published 30 November 2009)

A detailed α -decay study of the neutron-deficient isotope ^{181}Pb has been performed in the complete fusion reaction $^{40}\text{Ca} + ^{144}\text{Sm} \rightarrow ^{184}\text{Pb}^*$ at the velocity filter SHIP (GSI, Darmstadt). In comparison with the literature, more precise data have been deduced for the $I^\pi = (9/2^-)$ ground state in this nucleus, which is presumably based on the neutron $\nu h_{9/2}$ spherical orbital. Improved α -decay data were also measured for ^{180}Pb .

DOI: [10.1103/PhysRevC.80.054322](https://doi.org/10.1103/PhysRevC.80.054322)

PACS number(s): 23.60.+e, 23.20.Lv, 25.70.Jj, 27.70.+q

I. INTRODUCTION

The odd- A neutron-deficient isotopes $^{183-189}\text{Pb}$ are well known for the systematic appearance of two α and/or β -decaying states with spin and parity assignments of $I^\pi = 3/2^-$ for the ground state and of $13/2^+$ for the isomeric state [1,2]. These states are produced when an odd valence neutron occupies either the $3p_{3/2}$ or the $1i_{13/2}$ spherical orbital, respectively. Recent laser-spectroscopic studies at the mass separator ISOLDE confirmed these conclusions by measuring the magnetic moments and charge radii of both the $3/2^-$ ground state and the $13/2^+$ isomer in the isotopes $^{183-189}\text{Pb}$ [2–4]. A surprising observation for all these isotopes was the persistence of the $3/2^-$ ground state even down to the neutron number $N = 101$ (^{183}Pb), despite the fact that in the simple spherical shell model, the $3p_{3/2}$ orbital should already become empty by $N = 114$ (^{196}Pb). Thus it can be expected that below the neutron mid-shell at $N = 104$, the $1h_{9/2}$ or $2f_{7/2}$ neutron orbitals become important in the lead isotopes, as is observed in the light mercury and platinum nuclides, for example, in $^{175,177,179}\text{Hg}$ ($N = 95, 97, 99$) [5–9] or in ^{177}Pt ($N = 99$) [1,9,10].

The present work reports on a dedicated α -decay study of ^{181}Pb , for which more detailed information is now obtained in comparison to the previously known data. This isotope was previously studied in three experiments [11–13]. The studies [11,12] provided first, though relatively imprecise, α -decay data (see Table I), with no spin-parity assignment proposed. The latest work on this nucleus was published in a conference contribution [13], which suggested for the first time that, indeed, the ground state of ^{181}Pb should have a spin-parity assignment of $(9/2^-)$. However, no spectra, α -decay energy, or half-life information for ^{181}Pb was presented in Ref. [13].

II. EXPERIMENTAL SETUP

The isotopes ^{181}Pb and ^{180}Pb were produced in the $3n$ and $4n$ evaporation channels, respectively, of the complete

fusion reaction $^{40}\text{Ca} + ^{144}\text{Sm} \rightarrow ^{184}\text{Pb}^*$. Eight ^{144}Sm targets, each of 96.4% enrichment and $350 \mu\text{g}/\text{cm}^2$ thickness, were mounted on a wheel, rotating synchronously with the UNILAC macropulsing of 5 ms (“beam on”) and 15 ms (“beam off”). The targets were produced by evaporating the $^{144}\text{SmF}_3$ material onto a carbon backing of $40 \mu\text{g}/\text{cm}^2$ thickness and covered with a $10 \mu\text{g}/\text{cm}^2$ carbon layer to increase the radiative cooling and reduce the sputtering of the target material. Data were taken at several beam energies, covering the energy range of the $3n-4n$ evaporation channels.

After separation by the velocity filter SHIP [14], the evaporation residues (ERs) were implanted into a $300\text{-}\mu\text{m}$ -thick, $35 \times 80 \text{mm}^2$, 16-strip position-sensitive silicon detector (PSSD), where their subsequent particle decays were measured using standard implantation techniques [15].

The α -decay energy calibration of the PSSD was performed using known α lines of the isotopes $^{176-182}\text{Hg}$ (and their daughters), produced via the α , xn channels of the studied reaction. The broad energy range of $\sim 5300\text{--}6800$ keV and a small energy uncertainty for most of the α lines used for calibration allowed us to make a reliable extrapolation to the α -energy region of $6900\text{--}7300$ keV, relevant for $^{180,181}\text{Pb}$. A typical PSSD energy resolution of ~ 25 keV (FWHM) was achieved in the energy interval of $6000\text{--}7300$ keV. Since α -particle emission is a dominant decay mode of most of the nuclei produced in this reaction, the identification of nuclides was based on the observation of genetically correlated α -decay chains complemented with excitation function measurements.

A large-volume, fourfold segmented clover germanium detector was installed behind the PSSD to measure the energies of γ rays occurring within $5 \mu\text{s}$ of the detection of any particle decay in the PSSD. The energy threshold for the γ -ray registration was at ~ 15 keV; therefore we could not observe Hg L x rays ($E_\gamma \sim 9\text{--}12$ keV) in this experiment.

Three time-of-flight (TOF) detectors [16] were installed in front of the PSSD system, allowing us to distinguish the reaction products from the scattered beam particles. More

TABLE I. A comparison of α -decay energies E_α , half-life values $T_{1/2}$, and reduced α -decay widths δ_α^2 for $^{180,181}\text{Pb}$ from our measurement and from the earlier data. Note that no α -decay energy or half-life values were given for ^{181}Pb in Ref. [13].

Isotope	E_α (keV)	$T_{1/2}$ (ms)	δ_α^2 (keV)	Reference
^{181}Pb	7016(15)	36(2)	37(4)	Present work
	7044(15)	50^{+40}_{-30}	21^{+17}_{-13}	[11]
	7065(20)	45(20)	20(10)	[12]
^{180}Pb	7254 (10)	4.2 (5)	54 (8)	Present work
	7230(40)	4^{+4}_{-2}	68^{+70}_{-40}	[23]
	7250(15)	4.5(11)	52(14)	[24]

important, decay events in the PSSD could be distinguished from the implantation events by requiring an anticoincidence condition between the signals from the PSSD and from at least one of the TOF detectors.

III. EXPERIMENTAL RESULTS

A. Decay of ^{181}Pb

Figure 1(a) shows a part of the energy spectrum of α decays correlated with the ER implantation within the time interval $\Delta T(\text{ER}-\alpha_1) \leq 200$ ms. The shown data were collected during the “beam off” interval at the beam energy of 196(1) MeV in front of the target, at which most of the data for ^{181}Pb have been measured. Figure 1(b) shows the two-dimensional plot of α_1 - α_2 correlations for α_1 decays from Fig. 1(a) for the time interval $\Delta T(\alpha_1-\alpha_2) \leq 2$ s, while Fig. 1(c) shows the projection of Fig. 1(b) on the E_{α_1} axis.

Three main groups of α decays can be seen in Fig. 1(a): at 6911(15) keV, the broad group at ~ 6990 –7060 keV and a peak at 7083(15) keV. The α -line at 6911(15) keV is due to well-known decay of ^{182}Pb , see e.g. [17], which is also confirmed by the $\alpha_1(6911 \text{ keV})$ - $\alpha_2(6430(15) \text{ keV})$ correlations with its daughter nuclide ^{178}Hg , see Fig. 1(b).

We assign both the broad group at 6990–7060 keV and a peak at 7083(15) keV, seen in Figs. 1(a)–1(c), is due to α decay of ^{181}Pb . This is based on α - α correlations of these α decays with the known α decays of the daughter ^{177}Hg [$E_\alpha = 6582(15) \text{ keV}$, $T_{1/2} = 118(8) \text{ ms}$] and granddaughter ^{173}Pt [$E_\alpha = 6240(15) \text{ keV}$, $T_{1/2} = 430(40) \text{ ms}$] nuclides [see Fig. 1(b)]. Indeed, our measured data compare well with the tabulated values both for ^{177}Hg [$E_\alpha = 6580(8) \text{ keV}$, $T_{1/2} = 127.3(18) \text{ ms}$ [9]] and for ^{173}Pt [$E_\alpha = 6225(9) \text{ keV}$, $T_{1/2} = 376(11) \text{ ms}$] (see, e.g., Refs. [1,18]). In total, ~ 700 ER- α correlated events have been attributed to ^{181}Pb .

Figure 1(d) shows the two-dimensional α_1 - γ spectrum for α_1 events from Fig. 1(b) observed within the time interval $\Delta T(\alpha_1-\gamma) \leq 5 \mu\text{s}$. The group of four $\alpha(7016(15) \text{ keV})$ - $\gamma(77.2(5) \text{ keV})$ coincident events must therefore originate from ^{181}Pb . We interpret the 7016-keV α decay is due to the fine structure α decay of ^{181}Pb feeding the known excited state at 77 keV in ^{177}Hg [6]. As shown in Ref. [6], this state deexcites directly to the $7/2^-$ ground state of ^{177}Hg by a 77-keV transition. Unfortunately, as stated in Ref. [6], the multipolarity of the 77-keV transition could not be

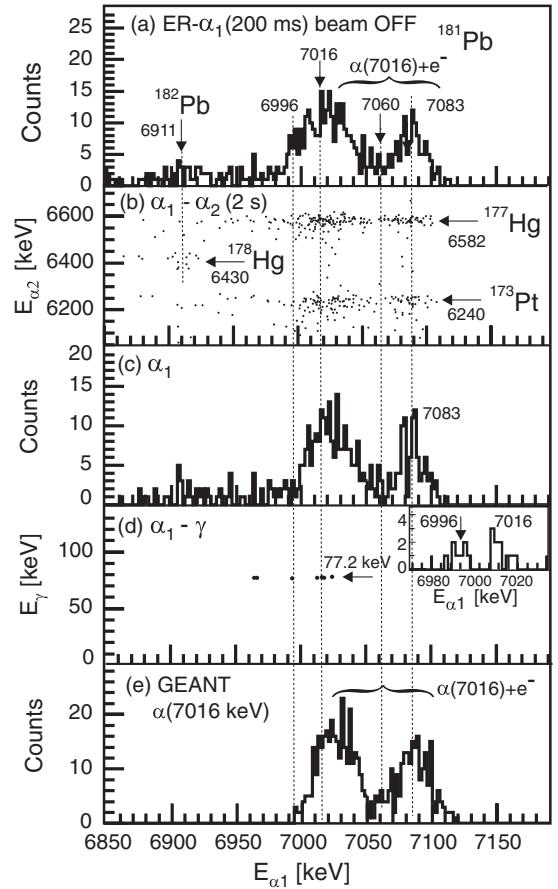


FIG. 1. (a) Part of the energy spectrum of α decays correlated with the ER implantation within the time interval of $\Delta T(\text{ER}-\alpha_1) \leq 200$ ms. The data were collected during the “beam off” interval. α -decay energies are given in keV. (b) The α - α correlation plot for the α_1 decays from (a), measured within the time interval of $\Delta T(\alpha_1-\alpha_2) \leq 2$ s. (c) Projection from (b) on the E_{α_1} axis. (d) E_{α_1} - E_γ spectrum for α_1 decays from (b) in coincidence with γ rays within $5 \mu\text{s}$. The inset shows the spectrum of α decays observed in coincidence with the 77.2 keV γ decays without any further conditions, except for the coincidence time interval of $5 \mu\text{s}$. (e) The result of the GEANT Monte Carlo simulation for the 7016-keV decay (see text for details).

unambiguously determined from their data, and based on a number of arguments, a tentative $M1$ multipolarity was suggested for this decay. In the following discussion, based on our data, we will confirm this inference experimentally.

We note in passing that our measured energy of 7016(15) keV differs from the energies of 7044(15) keV and 7065(20) keV reported for ^{181}Pb in the earlier studies of Ref. [11] and Ref. [12], respectively (see Table I).

The theoretical total conversion coefficient of the 77.2-keV transition is $\alpha_{\text{tot}}(M1) = 3.04$ [19]. As the energy of 77.2 keV is below the K -electron binding energy in Hg (83.1 keV [10]), the internal conversion from, predominantly, the L shell must be considered (L/M ratio is 4.3 [19]). This internal conversion results in conversion electrons with the energy of ~ 62.5 keV (L conversion) or ~ 73.7 keV for the weaker M conversion. Therefore the well-known effect of energy summing in a

silicon detector of the α -decay energy with the energy of the coincident conversion electron (and corresponding x rays) must be considered (see the detailed discussion in Refs. [20,21]). For example, if 62.5-keV conversion electrons are fully stopped in the PSSD, the full-energy peak at $\alpha(7016 \text{ keV}) + e^-(62.5 \text{ keV}) = 7079(15) \text{ keV}$ is produced, which is close to the α line at 7083(15) keV seen in Fig. 1(a). The weaker full-energy summing with the M electrons of 73.7 keV explains the broadening of this peak up to the energy of $\sim 7100 \text{ keV}$ [see Fig. 1(a)].

On the other hand, if such conversion electrons escape from the PSSD in the backward hemisphere, the partial $\alpha + e^-$ summing in the PSSD results in a higher energy tail of the 7016-keV α decay, also seen in our spectra. Collectively, both this tail and the full-energy summing peak at 7083 keV are denoted as $\alpha + e^-$ in Fig. 1. We also mention here explicitly that the energy summing with the Hg L x rays of $\sim 10\text{--}15 \text{ keV}$ also contributes to the observed spectra as x rays with such a low energy have a sizable probability of being fully or partially registered in the 300- μm -thick PSSD. These effects will be discussed further in the text.

By using the ER- α correlation analysis, half-life values of 37(4) ms and 35(3) ms have been deduced for the 7010–7060 and 7083-keV groups, respectively, which is consistent with both originating from the decay of the same state in ^{181}Pb . Based on all data in the 7010–7100 keV interval, the half-life value of 36(2) ms was deduced for the 7016-keV α decay of ^{181}Pb .

We note that if it exists, the full-energy “cross-over” $\alpha(7016(15) \text{ keV}) + \gamma(77.2 \text{ keV}) \sim 7093(15) \text{ keV}$ α decay of the 36(2)-ms state in ^{181}Pb would have an energy close to the energy of the full-energy $\alpha + e^-(M) + x$ ray summing peak, seen in Fig. 1(a). Therefore, for the (yet unobserved) 7093(15)-keV decay, we provide only an upper intensity limit of 5% relative to the main 7016-keV α decay.

To confirm this scenario, we performed GEANT simulations with a dedicated code, developed for the SHIP detection system [20]. In the simulations, a single 7016-keV decay of ^{181}Pb was considered, being in coincidence with the 77.2-keV $M1$ decay. For the sake of simplicity, in our simulations, we included only the L conversion of the 77.2-keV decay; however, the inclusion of a weaker M conversion will not change our conclusions. Also, the effect of the Hg L x rays at $\sim 10\text{--}15 \text{ keV}$ was considered in the simulations.

The result of such simulations for the 7016-keV α decay and related $\alpha(7016 \text{ keV}) + e^-(62.5 \text{ keV})$ summing effect is shown in Fig. 1(e). One can clearly see that the simulated spectrum is very similar in shape to the experimental spectrum in Fig. 1(c), which strengthens the proposed decay scheme.

However, we want also to point out two experimental facts. First of all, the comparison of Fig. 1(a) and Figs. 1(b) and 1(c) clearly shows that there is a weak “extra” peak at $\sim 6996 \text{ keV}$ in Fig. 1(a), which practically disappears (or becomes very weak) in Fig. 1(b) and Fig. 1(c). As mentioned earlier, Fig. 1(a) shows the result of ER- α correlations, in which no requirement of a subsequent correlation with the α decays of the daughter nuclides ^{177}Hg and ^{173}Pt was applied. Therefore the tentative 6996-keV decay in Fig. 1(a) can actually originate from some other nucleus, rather than from ^{181}Pb .

On the other hand, one $\alpha(6996 \text{ keV})\text{-}\gamma(77.2 \text{ keV})$ coincident event is seen in Fig. 1(d), similar to the 7016-keV decay of ^{181}Pb . This might indicate that the 6996-keV decay also belongs to ^{181}Pb , but it could also be that this particular coincident event is due to the lower energy tail from the 7016-keV decay. In this respect, we remind the reader here that Fig. 1(d) was produced from the ER- $[\alpha_1\text{-}\gamma]\text{-}\alpha_2$ correlation analysis, which reduces the number of such correlated events by at least a factor of 2, relative to the ER- $[\alpha_1\text{-}\gamma]$ analysis. The latter is due to $\sim 50\%$ PSSD detection efficiency for α decays. Therefore, to provide the full available statistics, the inset to Fig. 1(d) shows the α_1 spectrum, collected in coincidence with the 77.2-keV γ decays within the time interval of 5 μs without any extra conditions or correlations. Two peaks are clearly seen in the inset. One of them, with 10 counts, is the 7016-keV decay of ^{181}Pb , discussed earlier. The second decay, with eight counts, is at 6996(15) keV, which matches well to the position of the 6996-keV peak in Fig. 1(a). The half-life value of 30(10) ms for the latter events was deduced. However, as a word of caution, we reiterate here that only one out of these eight $\alpha(6996 \text{ keV})\text{-}\gamma(77 \text{ keV})$ coincident events in the inset remains in the ER- $[\alpha_1\text{-}\gamma]\text{-}\alpha_2$ correlation analysis in Fig. 1(d), instead of the expected four or five counts, as in the case of the 7016-keV decay. The 6996-keV decay will be discussed further in Sec. IV B.

By comparing the number of the α decays in the 6990–7060 keV group in Fig. 1(a) with the number of these decays in coincidence with the 77.2-keV γ ray in the inset to Fig. 1(d), after correction for the γ -registration efficiency, a total conversion coefficient of $\alpha_{\text{tot}}(77.2 \text{ keV}) = 2.7(9)$ was deduced. This confirms experimentally an $M1$ multipolarity, tentatively proposed in Ref. [6] for this transition, as the calculated total conversion coefficients are $\alpha_{\text{tot}}(E1) = 0.17$, $\alpha_{\text{tot}}(M1) = 3.04$, and $\alpha_{\text{tot}}(E2) = 16.7$ [19].

From the comparison of the number of $\alpha_1(6990\text{--}7100 \text{ keV})$ decays of ^{181}Pb in Fig. 1(a) and the number of $\alpha_1(6990\text{--}7100 \text{ keV})\text{-}\alpha_2(^{177}\text{Hg}, 6582 \text{ keV})$ correlated decays in Fig. 1(b), an α -branching ratio of $b_\alpha = 100\%$ was deduced for ^{177}Hg with a precision of 5%, which is determined by the statistical uncertainty. This value is larger and more precise than the previously reported estimate of $b_\alpha \sim 85\%$ (see Refs. [9,22]).

B. α decay of ^{180}Pb

The first identification of ^{180}Pb was performed by using a rapidly rotating wheel system [23]. An α -decay energy of 7230(40) keV and a half-life value of 4_{-2}^{+4} ms were deduced based on a few registered events (see Table I). The subsequent work [24] at the fragment mass analyser collected approximately 10 decay events of ^{180}Pb (see Fig. 1 of Ref. [24]). Improved values of $E_\alpha = 7250(15) \text{ keV}$ and $T_{1/2} = 4.5(11) \text{ ms}$ were deduced.

In our experiment, we collected approximately 100 α -decay events of ^{180}Pb , which could reliably be identified based on their correlations with well-known α decays of daughter ^{176}Hg and granddaughter ^{172}Pt nuclides. Our measured values for ^{176}Hg are $E_\alpha = 6760(15) \text{ keV}$, $T_{1/2} = 20(3) \text{ ms}$; those for ^{172}Pt are $E_\alpha = 6324(15) \text{ keV}$, $T_{1/2} = 100(20) \text{ ms}$. These values

B. Tentative 6996-keV α decay

Finally, as far as the tentative 6996-keV α decay is concerned, we also mention a possible scenario in which the 6996-keV α decay actually originates from another α -decaying state in ^{181}Pb with a half-life similar to that of the $9/2^-$ state decaying by the 7016-keV decay. Such a state could then have a spin-parity assignment of either $13/2^+$ or $3/2^-$ as such α -decaying states are well known in the heavier odd- A isotopes. For example, in ^{183}Pb , the $13/2^+$ and $3/2^-$ α -decaying states have comparable half-life values of 415(20) ms and 535(30) ms, respectively [7], with the $13/2^+$ state lying only 79(6) keV above the $3/2^-$ ground state. However, as mentioned earlier, the $13/2^+$ assignment for this state is highly unlikely because of the half-life considerations, and thus we rule out this possibility and discuss subsequently the possible $3/2^-$ assignment for this state.

The observed 6996–77.2 keV α - γ coincidences might indicate that the 6996-keV decay actually proceeds from the state ~ 20 keV below the 36(2)-ms α -decaying state; thus the former state would then become the ground state in ^{181}Pb . In this case, the 6996-keV decay would be a $\Delta L = 4$, $3/2^- \rightarrow 9/2^-$ α decay, which would need to compete with a direct, $\Delta L = 2$, 7071(15)-keV α decay to the $7/2^-$ ground state of ^{177}Hg . Clearly the latter decay should be more favorable, both because of its larger energy and lower ΔL value. Unfortunately, such a decay would be hidden by the summing peak at 7083 keV (see Fig. 1), and thus we cannot quantify this scenario.

To summarize this tentative discussion, given the scarce data for the 6996-keV α decay, it is presently impossible to discuss this decay unambiguously. Much higher statistics

would be required to clarify if the 6996-keV decay belongs to ^{181}Pb and from which state it originates.

V. CONCLUSIONS

A detailed α -decay study of isotope ^{181}Pb was performed in the complete fusion reaction of ^{40}Ca ions with the ^{144}Sm target. The relatively large number of decays collected in our experiment, along with the efficient and versatile detection system, allowed us to identify the fine-structure 7016-keV α decay of this nucleus. Based on the much more detailed decay pattern of ^{181}Pb (in comparison with previous Refs. [11,12]) and on the properties of the states in the daughter nucleus ^{177}Hg , it is shown that an α -decaying state with a spin-parity assignment of $I^\pi = 9/2^-$ is present. The state is based presumably on the spherical $vh_{9/2}$ orbital. No unambiguous evidence for the $3/2^-$ or $13/2^+$ states, which are typically seen in the heavier odd- A Pb isotopes, was found in our data.

ACKNOWLEDGMENTS

We thank the UNILAC staff for providing the stable and high-intensity ^{40}Ca beams. This work was supported by FWO-Vlaanderen (Belgium) [Grant No. GOA/2004/03 (BOF–K. U. Leuven)], by the “Interuniversity Attraction Poles Programme–Belgian State Belgian Science Policy” (BriX network P6/23), by the European Commission within the Sixth Framework Programme through I3-EURONS (Contract No. RII3-CT-2004-506065), and by the UK Science and Technology Facilities Council. S.A. and Š.Š. were supported by the Slovak Research and Development Agency under Contract No. APVV-20-006205.

-
- [1] Evaluated Nuclear Structure Data File (ENSDF), <http://www.nndc.bnl.gov/ensdf/>.
- [2] M. D. Seliverstov *et al.*, *Eur. Phys. J. A* **41**, 315 (2009).
- [3] H. De Witte *et al.*, *Phys. Rev. Lett.* **98**, 112502 (2007).
- [4] J. Sauvage *et al.*, *Eur. Phys. J. A* **39**, 33 (2009).
- [5] D. O’Donnell *et al.*, *Phys. Rev. C* **79**, 051304(R) (2009).
- [6] A. Melerangi *et al.*, *Phys. Rev. C* **68**, 041301(R) (2003).
- [7] D. G. Jenkins *et al.*, *Phys. Rev. C* **66**, 011301(R) (2002).
- [8] F. G. Kondev *et al.*, *Phys. Lett.* **B528**, 221 (2002).
- [9] F. G. Kondev, *Nucl. Data Sheets* **98**, 801 (2003).
- [10] R. B. Firestone *et al.*, *Table of Isotopes*, 8th ed. (John Wiley, New York, 1996).
- [11] K. S. Toth, D. M. Moltz, and J. D. Robertson, *Phys. Rev. C* **39**, 1150 (1989).
- [12] K. S. Toth *et al.*, *Phys. Rev. C* **53**, 2513 (1996).
- [13] M. P. Carpenter, F. G. Kondev, and R. V. F. Janssens, *J. Phys. G: Nucl. Part. Phys.* **31**, S1599 (2005).
- [14] G. Münzenberg *et al.*, *Nucl. Instrum. Methods* **161**, 65 (1979).
- [15] S. Hofmann *et al.*, *Z. Phys. A* **291**, 53 (1979); S. Hofmann and G. Münzenberg, *Rev. Mod. Phys.* **72**, 733 (2000).
- [16] Š. Šaro *et al.*, *Nucl. Instrum. Methods A* **381**, 520 (1996).
- [17] D. G. Jenkins *et al.*, *Phys. Rev. C* **62**, 021302(R) (2000).
- [18] R. D. Page *et al.*, *Phys. Rev. C* **53**, 660 (1996).
- [19] T. Kibédi *et al.*, *Nucl. Instrum. Methods A* **589**, 202 (2008); Conversion Coefficients Calculator BrIcc v2.2a, <http://www.rpsphsye.anu.edu.au/nuclear/briccc/>.
- [20] A. N. Andreyev *et al.*, *Nucl. Instrum. Methods A* **533**, 409 (2004).
- [21] F. P. Heßberger *et al.*, *Nucl. Instrum. Methods A* **274**, 522 (1989).
- [22] E. Hagberg *et al.*, *Nucl. Phys.* **A318**, 29 (1979).
- [23] K. S. Toth *et al.*, *Z. Phys. A* **355**, 225 (1996).
- [24] K. S. Toth *et al.*, *Phys. Rev. C* **60**, 011302(R) (1999).
- [25] J. R. H. Schneider *et al.*, *Z. Phys. A* **312**, 21 (1983); J. R. H. Schneider, Report No. GSI-84-3, 1984.
- [26] M. S. Basunia, *Nucl. Data Sheets* **107**, 791 (2006).
- [27] M. Danchev *et al.*, *Phys. Rev. C* **67**, 014312 (2003).
- [28] J. O. Rasmussen, *Phys. Rev.* **113**, 1593 (1959).